# Spatio-temporal distribution of water availability in Karnali-Mohana Basin, Western Nepal: Hydrological model development using multi-site calibration approach (Part-A)

Vishnu Prasad Pandey[1,*], Sanita Dhaubanjar[1], Luna Bharati[1], Bhesh Raj Thapa[1]

[1]*International Water Management Institute (IWMI), Nepal Office, Lalitpur, Nepal*

**Corresponding Author: v.pandey@cgiar.org*

## Abstract

*Study region*: Karnali-Mohana (KarMo) river basin, Western Nepal.

*Study focus*: This study has developed a hydrological model using multi-site calibration approach for a large basin, the Karnali-Mohana (KarMo) in Western Nepal, which has a lot of potential for water resources development and contribute to the national prosperity. It further applies the model to characterize hydrology and water resources availability across spatio-temporal scales to enhance understanding on water availability and potential uses. The newly developed hydrological model in Soil and Water Assessment Tool (SWAT) is capable of reproducing the hydrological pattern, the average flows, and the flow duration curve at the outlet of the basin and five major sub-basins.

*New hydrological insights for this region*: The model simulated results showed that about 34% of average annual precipitation in the KarMo basin is lost as evapotranspiration, but with a large spatio-temporal heterogeneity. The Hills and Tarai are relatively wetter than the Mountains. The average annual flow volume at the basin outlet is estimated as 46,250 million-cubic-meters (MCM). The hydrological characterization made in this study are further used for climate change impact assessment (Part-B in the same journal), environmental flows assessment and evaluating trade-offs among various water development pathways, which are published elsewhere. This model developed in this study, therefore, has potential to contribute for strategic planning and sustainable management of water resources to fuel the country's prosperity.

***Keywords:*** *Hydrology; Karnali; Mohana; SWAT; Water Resources; Western Nepal*

28

## 1. Introduction

Hydrological observations at a high spatial and temporal resolution is resource-intensive. Therefore, many countries are yet to reach to that level even though the coverage is improving over the years. Even if the coverage is adequate, developing hydrological simulation models can provide reliable estimates for water yield and availability in a basin over a wide range of input watershed conditions under a variety of climatic scenarios. Spatial explicit hydrological models are particularly useful to evaluate impacts under various scenarios on water availability and distribution (Thapa et al., 2017). Furthermore, the simulation models provide an excellent platform for evaluating various options for water and environmental planning. Such information is crucial for policy/decision-makers, implementing agencies, and practitioners to quantify different types of threats to water and environmental security; design policies and programmes; and devise strategies for better allocation, utilization, and management of freshwater resources (Sunsnik, 2010; Thapa et al., 2017) as well as environmental protection for the country's prosperity. The need for such a modelling system is stimulated and sometimes even enforced by many activities required by river basin planning and management (Halwatura and Najim, 2013). For example, water balance studies in Iran are customary for allocating budgets to water resource policies and projects (Ghandhari and Alavi-Moghaddam, 2011). It is therefore imperative to develop hydrological models for the basins of interest and apply to characterize spatio-temporal distribution of hydrology and water resources.

Western Nepal is generally perceived as one of the poorest regions in the country with low literacy, limited development, high poverty, very little market access, and similar disadvantages (Pandey et al., 2018). Such perceptions reflect inadequate understanding of the untapped natural resources potential that the region has. The Karnali and Mahakali basins in the region account for 28% of total available water resources in Nepal (Pandey et al., 2010). Natural resources are also abundant and tourism potentials are also high. With steep slopes and meandering rivers, Western Nepal also offers tremendous potential for hydropower development. There are 150 identified hydropower projects of various types, including 19 storage projects, under various stages of development, with proposed installed capacity ranging from 0.5 to 6,720 megawatts (MW) (IWMI, 2018). Total estimated installed capacity of all these projects is more than 21,000 MW. Implementing all these projects will contribute to energy security and fuel economic growth for national prosperity. Mohana basin, with the catchment area of 3,730 $km^2$; is located in the south of the Karnali basin; originates from Nepali Churia hills; and varies in topography from 113 to 1,928 masl. The Mohana basin hosts at least 11 irrigation projects under operation with a total net command area of 26,583 hectares (ha). The net command area of the 11 projects vary from 155 ha to 15,800 ha. An endangered species of Ganges River dolphin (Platanista gangetica) were recently reported to inhabit the Mohana river. It is therefore imperative to maintain a healthy aquatic environment in order to protect an endangered species. Despite having tremendous potentials of the region, adequate development and management of water resources is yet to gain momentum for various reasons, including inadequate scientific understanding on spatio-temporal distributional of water availability.

There are several studies focusing on hydrological modelling at Nepalese watersheds (Babel et al., 2014; Bajracharya et al., 2018; Bharati et al., 2014), however only one (Dhami et al., 2018) focuses on the Karnali basin in the western Nepal, and none in the Karnali-Mohana (KarMo) basin (Fig. 1). Even the one focusing on the Karnali has used limited number of stations for model calibration, and has not characterized hydrology adequately from spatio-temporal distribution perspective. Furthermore, various hydrological models have been used over the time to reproduce hydrological patterns over a watershed. Some of them are empirical (e.g. Tank Model, Sugawara 1979), while others are lumped (e.g., HEC-HMS, Feldman, 2000), semi-distributed (e.g., SWAT, Arnold et al., 1998; Srinivasan et al., 1998), or fully distributed (e.g., BTOPMC, Takeuchi et al. 1999). However, application for a specific purpose and for a typical study area depends upon several factors. The Soil and Water Assessment Tool (SWAT) is widely used at different spatial scales to simulate hydrology, soil erosion, sedimentation, and impacts studies, among others (Aryal et al., 2018; Bajracharya et al., 2018; Bharati et al., 2016; Devkota and Gyawali, 2015; Jeong et al., 2010). The SWAT model is therefore selected in this study for hydrological simulation of the study basin.

Many studies use SWAT model with calibration at only the outlet to characterize hydrology. However, in highly heterogeneous large basins such as KarMo, with basin area of 49,892 $km^2$, it needs to be calibrated at multiple sites should we expect the model truly reproduce spatial heterogeneity in hydrological processes. Recent literatures (e.g., Hasan and Pradhanang, 2017; Nkiaka et al., 2018; Pandey et al., 2019) also put emphasis on multi-variable multi-site calibration approach considering the need to better represent spatial heterogeneity within the modelled watershed. This study therefore aims to develop a hydrological model in SWAT environment for the KarMo basin with multi-site calibration approach, and then apply it to characterize spatio-temporal distribution in water availability across the basin. The fully calibrated and validated hydrological model is then used for climate change impact assessment (in forthcoming concurrent paper), environmental flows assessment and evaluating trade-offs among various water development pathways (Pakhtigian et al., 2019).

## 2. STUDY AREA

The KarMo basin area above Nepal-India border covers 49,892 km$^2$, of which 6.9% falls in the Tibetan Plateau, China and the rest in Western Nepal. The Karnali river originates in Tibetan Plateau and Trans-Himalayas (TrH) at altitudes of 5,500 m to 7,726m and flows through Mountains (Mnt), Hills (Hil), and Indo-Gangetic Plain (IGP) as shown in Fig. 1 and Fig. 2. The river spans 230 km from the northern basin boundary to the *Chisapani* station (Q280) in the south (length of mainstream Karnali river). The smaller Mohana river originates in Churia hills of Nepal, descends through the Terai, and drains into Karnali river at the Nepal-India border. The watershed area of Mohana alone above the Nepal-India border is 3,730 km$^2$. Karnali has a dendritic stream network in most of the areas while Mohana comprises of parallel stream network characterized by flash floods in the monsoon. Major tributaries of the Karnali river are Bheri, Thuli Bheri, Seti, Mugu Karnali and Humla Karnali.

The KarMo basin has a wide spatial heterogeneity in biophysical and climatic characteristics. The topographical variation ranges from 69 – 7,726 meters above mean sea level (masl) (Fig. 1). There are nine generic land use/cover classes with dominance of forest cover (about one-third of the basin area) (Fig. 3a), and 21 soil types with dominance of Gleic Leptosol (34.2% of basin area) (Fig. 3b) in the basin. Hydro-climatic conditions also vary, as evident from data at 36 meteorological stations from Department of Hydrology and Meteorology (DHM), and six grid points from Indian Meteorological Department (IMD) (Fig. 1).

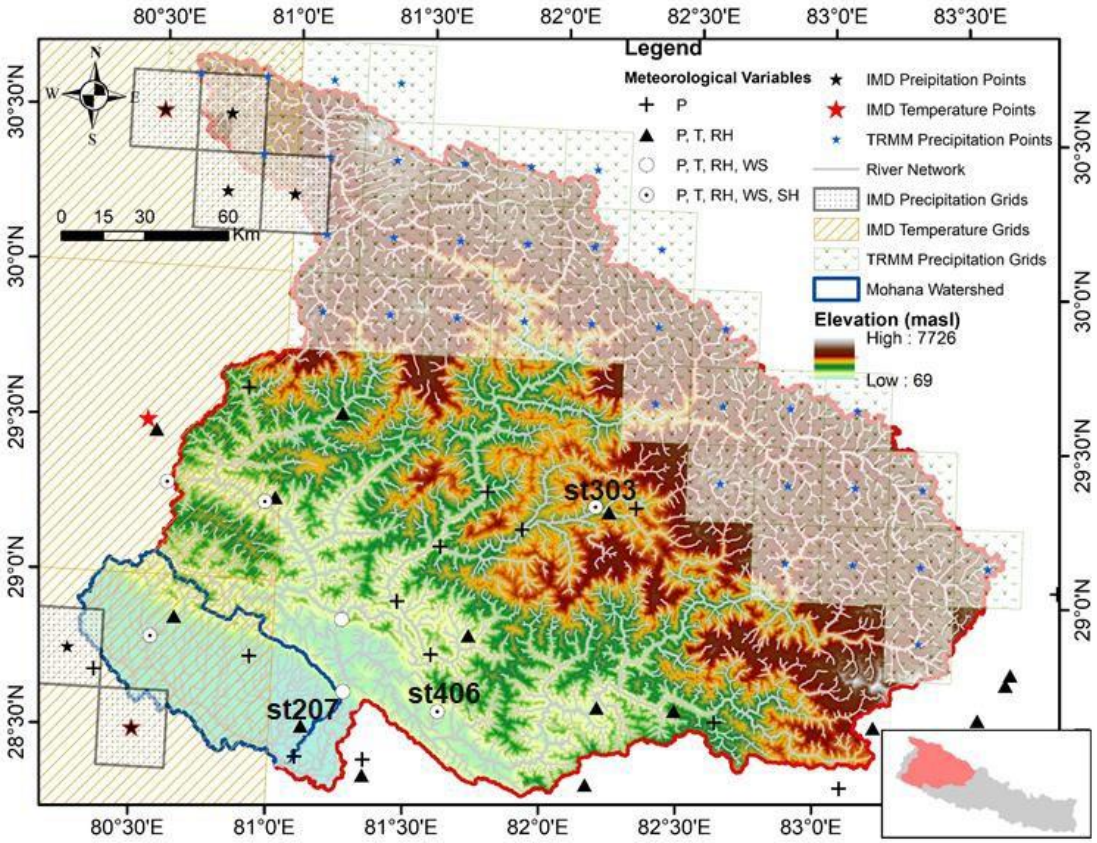


**Figure 1**: Study area: location, topographical variation, and meteorological stations/grids

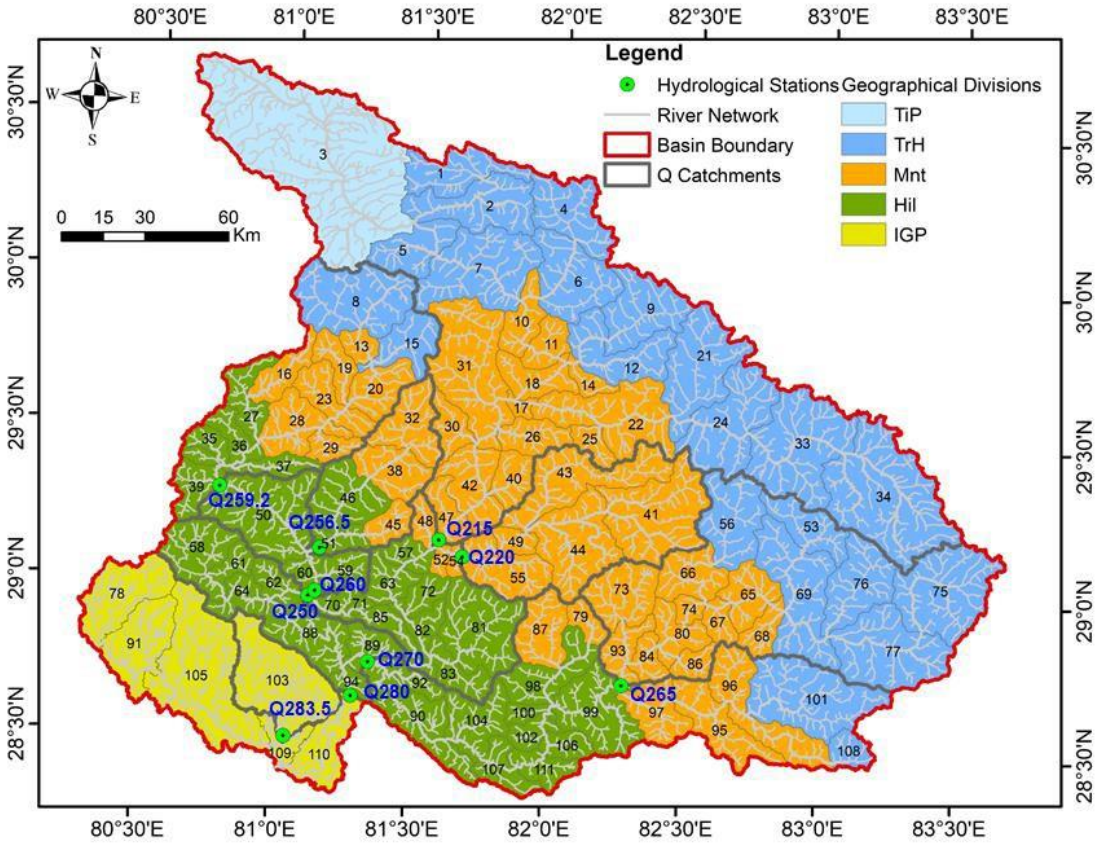


**Figure 2**: SWAT sub-watersheds and model calibration stations along with geographical divisions of the KarMo basin. TiP is Tibetan Plateau; TrH is Trans-Himalaya; Mnt is Mountain; Hil is Hill; IGP is Indo-Gangetic Plain; Q-catchments are catchments above gauging stations.

A database compiled by the Digo Jal Bikas project (http://djb.iwmi.org/) shows that there are 127 hydropower projects ranging from 0.5 to 1,003 megawatts (MW) at various stages of development in the KarMo basin. Similarly, 48 existing and one under-construction irrigation projects are also located within the basin. The net command area of these projects range from 100 – 98,026 ha. There are ample prospects for future water resources development activities in the basin, including tourism, and therefore, understanding spatio-temporal distribution in water availability and implications of climate change (CC) is important for the stakeholders across various water-use sectors.

## 3. METHODOLOGY AND DATA

Fig. 4 depicts the methodological flowchart and following sub-sections describe them in detail.

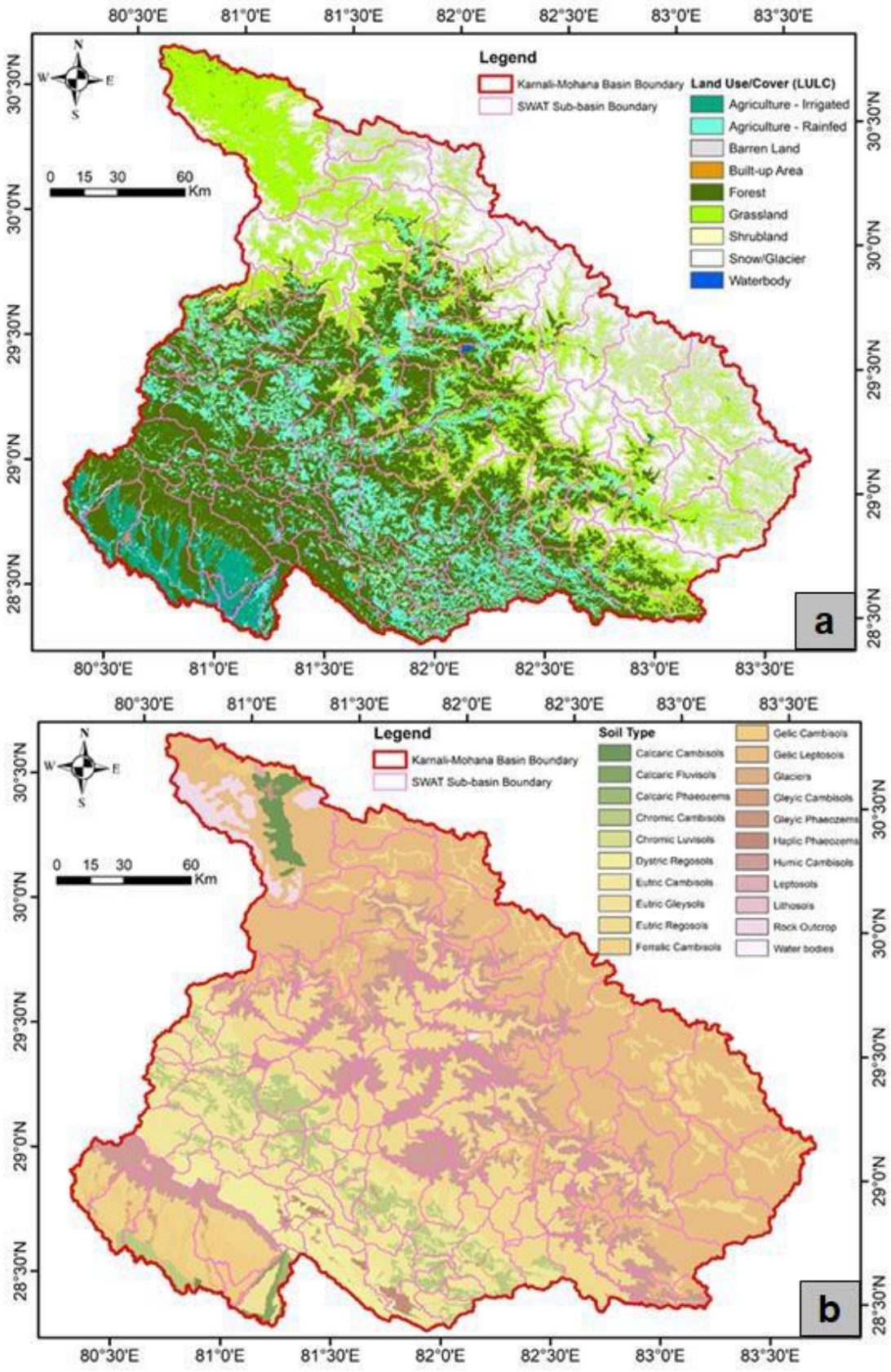


**Figure 3**: Land use/cover (a) and soil type (b) distribution within Karnali-Mohana basin (Source: ICIMOD (2010) and ESA (2015) for land use/cover and Dijkshoorn and Huting (2009) for soil type)

### 3.1 Model overview

SWAT is a process-based hydrological model capable of simulating hydrology, sediment transport, vegetation growth and management practices in complex basins with varying soils, land use/cover and management conditions (Arnold et al., 1998; Srinivasan et al., 1998). Conceptually, SWAT divides a basin into sub-basins and further into Hydrologic Response Units (HRUs). A stream channel connects the sub-basins. Each HRU represents a unique combination of a soil, land use/cover and slope type within a sub-watershed. The hydrologic cycle as simulated by SWAT is based on the water balance equation:

$$SW_t = SW_o + \sum_{i=1}^{n} (R_{day} - Q_{surf} - E_a - w_{seep} - Q_{gw})$$

Where, $SW_t$ is Final soil water content (mm); $SW_0$ is Initial soil water content (mm); t is Time in days; $R_{day}$ is Amount of precipitation on day i (mm); $Q_{surf}$ is Amount of surface runoff on day i (mm); $E_a$ is Amount of evapotranspiration on day i (mm); $w_{seep}$ is Amount of percolation on day i (mm); and $Q_{gw}$ is Amount of return flow on day i (mm).

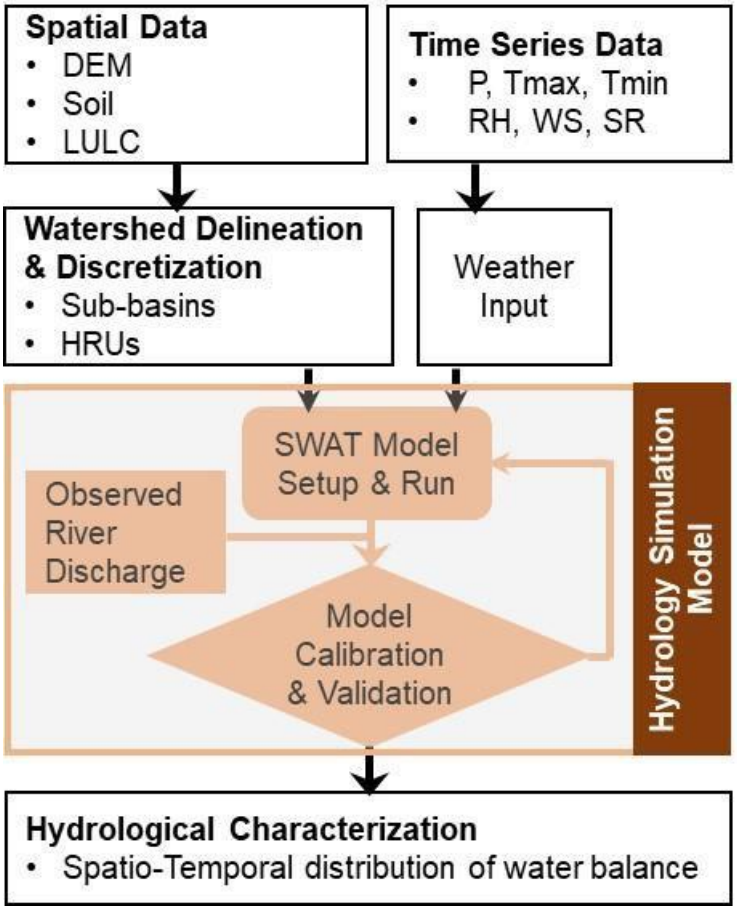


**Figure 4**: Methodological framework for developing and applying hydrological model for hydrological characterization of the Karnali-Mohana (KarMo) basin. DEM is Digital Elevation Model; LULC is land use/cover; HRU is hydrological response unit; P is precipitation (in mm); T is temperature (in °C); RH is relative humidity (in fraction); WS is wind speed (in m/s); and SR is solar radiation ($MJ/m^2/day$).

SWAT simulates water balance at the HRU level and then aggregates into sub-basin level. Subdivision of the basin into HRUs enables it to reflect differences in evapotranspiration for various land cover crops and soils. Runoff is predicted separately for each sub-basin and routed along the stream channel to obtain total runoff at the basin outlet. Such spatial representation increases accuracy and gives a much better physical description of the water balance. Arnold et al. (1998) and Srinivasan et al. (1998) provide descriptions of the model.

### 3.2 Model set-up

Spatially distributed data for topography (Fig. 1), land use/cover (Fig. 3a), and soil (Fig. 3b) were used as inputs to set-up the model. Daily time series of observed meteorological variables at various locations (Fig. 1) were taken from secondary sources as indicated in Table 1. The climatic data were then pre-processed to convert into SWAT-compatible format. Precipitation and temperature were used in the same unit as collected from DHM. In case of relative humidity, two sets of observed data per day (morning and evening) were averaged and converted into a fraction before feeding into SWAT. Daily sunshine hours were converted into solar radiation ($MJ/m^2/day$) using Angstrom-Prescott (AP) model (Allen et al., 1998). Daily wind speed data available in km/hr was converted into m/s before using with SWAT.

**Table 1**: Data type, properties and sources used in this study

| Dataset [Unit] | Data Type | Data Description/ Properties | Data Source | Resolution (Time frame) |
|---|---|---|---|---|
| Terrain [m] | Spatial grids | Digital Elevation Model (DEM) | NASA JPL (2009) | 30m x 30m grids (for 2009) |
| Soil [-] | Spatial vectors | Soil classification and physical properties (e.g., texture, porosity, field capacity, wilting point, saturated conductivity and soil depth) | Dijkshoorn and Huting (2009) | 1:1 million map (from multiple years) |
| Land use/cover (LULC) [-] | Spatial grids | Landsat land use/cover classification (9 classes) | ICIMOD (2010); ESA (2015) | 30m x 30m grids (for 2010) |
| Precipitation [mm] | Time-series and spatial grids | Daily observed precipitation | DHM; Indian Meteorological Department (IMD), and TRMM | 36 DHM stations; 6 IMD stations, (1981-2013); and 36 TRMM grids (0.25° x 0.25°) |
| Temperature [°C] | Time-series | Daily observed minimum and maximum temperature | DHM, Nepal<br>IMD, India | 16 DHM stations and 3 IMD stations (1981-2013) |
| Relative humidity [-] | Time-series | Daily observed relative humidity in morning and evening | DHM, Nepal | 15 stations (1981-2013) |
| Sunshine hours [hrs] | Time-series | Daily observed sunshine hours | DHM, Nepal | 5 stations (1981-2013) |
| Wind speed [m/s] | Time-series | Daily observed mean wind speed | DHM, Nepal | 7 stations (1981-2013) |
| River discharge [$m^3/s$] | Time-series | Daily observed streamflow | DHM, Nepal | 10 stations (1981-2013) |

*DHM is Department of Hydrology and Meteorology, Nepal; TRMM is Tropical Rainfall Measuring Mission; NASA is National Aeronautics and space Administration (NASA); IMD is Indian Meteorological Department.*

ArcSWAT2012 was used as a platform to set-up SWAT model. A threshold area of 3,000 ha was defined to generate river network. To capture spatial heterogeneity, the basin was divided into 111 sub-basins with areas ranging from 44 – 3,183 $km^2$ and HRU area from 100 – 1,000 $km^2$. Next, 2,122 HRUs were defined using land use/cover (2%), soil type (5%) and three slope classes (0 – 15%; 15-30%; and more than 30%). Ten elevation bands at an interval of 500m were defined to model snowmelt as well as orographic distribution of temperature and precipitation. Weather input was fed in the form of daily precipitation (78 stations), maximum and minimum temperatures (19 stations), relative humidity (15 stations), wind speed (7 stations) and sunshine hours (5 stations) (Annex-2; Fig. 1). SCS curve number method was used to estimate surface runoff, where daily curve number was estimated as a function of soil

moisture. The Penman-Monteith method was used to estimate potential evapotranspiration (PET). Variable storage method was adopted to route channel flow. No point source discharge was defined. Eight existing irrigation projects were included as water abstraction points in the setup. Rice-Wheat-Maize cropping pattern was assigned as the representative cropping pattern in the sub-basins of Mohana.

### 3.3 Sensitivity analysis

Sensitivity analysis was carried out using SWAT-CUP, which combines the Latin Hypercube (LH) and one-factor-at-a-time (OAT) sampling (Van Griensven, 2005). In the OAT approach, one parameter values are changed at a time while keeping others constant. Twenty (20) model parameters (Table 2) were shortlisted for sensitivity analysis based on literature review (e.g., Bharati et al., 2014; Shrestha et al., 2016; Bajracharya et al., 2018; Dhami et al., 2019; Pandey et al., 2019) and prior experience of the modelling team. For each calibration point, sensitivity of parameters for the sub-watersheds upstream of the point is expected differ. Some parameters could be highly sensitive in some sub-watersheds, while other parameters in other sub-watersheds. Therefore, it is not possible to assign a sensitivity rank across the entire basin to the parameters.

### 3.4 Model calibration and validation

Multi-station and multi-variable calibration approach was adopted to better represent spatial heterogeneity in the KarMo basin. The calibration and validation was first performed at upstream stations and then gradually moved towards downstream stations. Once calibrated, sub-basins above upstream stations were locked and model parameters were not changed. The SWAT model was calibrated and validated against daily and monthly observed flows at 10 hydrological stations shown in Fig. 2 (please refer Annex-1 for details of the stations) along five major tributaries in KarMo basin. Three stations (Q215; Q250 and Q280) are in the Karnali-main river, two (Q265 and Q270) in Bheri; three (Q259.2, Q256.5 and Q260) in Seti; one (Q 220) in Tila; one (Q 283.3) in Mohana. Stations were selected to represent upstream downstream conditions in each tributary to analyse spatial variation in model performance.

The calibrated and validation periods considered are 1995-2002 and 2003-2009, respectively, for six stations (i.e., Q220, Q250, Q259.2, Q265, Q270, A280) whereas varying periods for other stations based on availability of good quality and continuous time series (Annex-2). A warm up period of three years was used to develop appropriate soil and groundwater conditions. The model was calibrated in three stages: i) Sensitivity analysis; ii) Auto-calibration; and iii) Manual calibration. After sensitivity analysis, SWAT-CUP was used for auto-calibration. The model was run for 1,000 iterations initially to narrow down the range of values for the sensitive parameters. Then auto-calibration results were further subjected to manual calibration based on knowledge of the basin.

During manual calibration, adjustments were made firstly to those parameters which were most sensitive and then moving to the less sensitive ones. Observed and simulated flows were visually compared in terms of the hydrographs (peak, time to peak, shape of the hydrograph and baseflow); scatter plots; flow duration curve; statistical parameters, and water accumulation to evaluate and improve model performance during manual calibration. Following statistical parameters were considered: mean, coefficient of determination ($R^2$), Nash-Sutcliffe efficiency (NSE), and percent bias (PBIAS). Details of these methods are available in Nash and Sutcliffe (1970), Gupta et al. (1999), and Moriasi et al. (2007). The model performance was evaluated for both monthly and daily simulations. Due care was given to keep physically-based parameters within a reasonable range (Table 2) throughout the calibration process.

**Table 2**: SWAT parameters selected for multi-site model calibration of Karnali-Mohana basin

| Parameter* | Definition | Unit | Process (Data file)* | Level* | Range | Initial value |
|---|---|---|---|---|---|---|
| ALPHA_BF | Baseflow recession constant | days | Groundwater (.gw) | HRU | 0 – 1 | 0.048 |
| GW_DELAY | Delay time for aquifer recharge | days | Groundwater (.gw) | HRU | 0 – 500 | 31 |
| GW_REVAP | Groundwater revap coefficient | - | Groundwater (.gw) | HRU | 0.02 – 0.2 | 0.02 |
| SHALLST | Initial depth of water in shallow aquifer | mm | Groundwater (.gw) | HRU | 0 – 50000 | 1000 |
| GWQMN | Threshold depth of water in shallow aquifer for groundwater return flow to occur | mm | Soil (.gw) | HRU | 0 – 5000 | 1000 |
| RCHRG_DP | Deep aquifer percolation fraction | - | Groundwater (.gw) | HRU | 0 – 1 | 0.05 |
| REVAPMN | Threshold depth of water in shallow aquifer for revap to occur | mm | Groundwater (.gw) | HRU | 0 – 500 | 750 |
| CANMX | Maximum canopy storage | mm | Runoff (.hru) | HRU | 0 – 100 | 0 |
| EPCO | Plant uptake compensation factor | - | Evaporation (.hru) | HRU | 0 – 1 | 1 |
| ESCO | Soil evaporation compensation factor | - | Evaporation (.hru) | HRU | 0 – 1 | 0.95 |
| LAT_TTIME | Lateral flow travel time | days | HRU (.hru) | HRU | 0 – 180 | 0 |
| SOL_AWC | Available water storage capacity of the soil layer | - | Soil (.sol) | HRU | 0 – 1 | Varies |
| SOL_K | Saturated soil conductivity | mm/hr | Soil (.sol) | HRU | 0 – 2000 | Varies |
| SOL_Z | Depth from soil surface to bottom of layer | mm | Soil (.sol) | HRU | 0 – 3500 | Varies |
| CN2 | SCS runoff curve number for moisture condition II | - | Runoff (.mgt) | HRU | 35 – 98 | Varies |
| CH_K2 | Effectivity hydraulic conductivity in main channel alluvium | mm/hr | Channel (.rte) | Reach | 0 – 500 | 0 |

| | | | | | | |
|---|---|---|---|---|---|---|
| CH_N2 | Manning's "n" value for the main channel | - | Channel (.rte) | Reach | 0 – 1 | 0.014 |
| TLAPS | Temperature lapse rate | °C/km | Topographic effect (.sub) | Sub-basin | -10 – 10 | -5.6 |
| PLAPS | Precipitation lapse rate | mm/km | Topographic effect (.sub) | Sub-basin | -1000 – 1000 | 0 |
| CH_N1 | Manning's "n" value for the tributary channel | - | Runoff (.sub) | Sub-basin | 0.01-30 | 0.014 |

*For detailed explanation of the parameters, please refer to Arnold et al. (2012).*

### 3.5 Data and sources

Both geo-spatial and time-series data reflecting biophysical, hydro-climatic and future climatic contexts are required in this study. They were collected from local and global sources as described in Table 1.

## 4. RESULTS AND DISCUSSION

### 4.1 Evaluation of SWAT model

The SWAT model is calibrated and validated at 10 hydrological stations (Fig. 2) spread across five major tributaries of the KarMo basin, namely, Karnali-main, Bheri, Seti, Tila, and Mohana. The calibrated parameter values are listed in Table 3. The number of parameters calibrated varies across the sub-basins, from 6 (in Q280) to 18 (in Q283.5), depending upon their sensitivity (Table 3). The sensitive parameters were not consistent across the sub-basins. However, baseflow recession factor (ALPHA_BF), curve number (CN2), and groundwater delay (GW_DELAY) were among the most sensitive parameters for most of the sub-basins. The level of influence of those parameters to the results, however, varied from one to another sub-basin. The model under-estimated baseflow with default SWAT parameter values. Therefore, CN2 was fine-tuned to increase infiltration and subsequent increase in groundwater contribution to the baseflow. Values of ALPHA_BF was adjusted based on visual inspection of shape of the recession limb of hydrograph. Similarly, other flow-related parameters such as soil depth (SOL_Z, available capacity of soil moisture (SOL_AWC), saturated hydraulic conductivity (SOL_K), soil evaporation compensation factor (ESCO), and lateral flow travel time (LATTIME), among others, were adjusted to match simulated and observed flows as well as reasonably approximate the water balance components. Defining elevation bands allowed for variable temperature laps rate (TLAPS) and precipitation laps rate (PLAPS) to account for spatial distribution of temperature and precipitation.

The model performance within major tributaries is discussed hereunder. At each station, a summary plot as shown in Fig. 5 was prepared to compare fit of hydrological simulation at daily and monthly scales, scattering of observed versus simulated points from the mean, model capability to reproduce flow duration curve (FDC), and model performance indicators.

#### *4.1.1 Karnali-main stations*

Three hydrological stations located in upstream, mid-stream, and downstream points of the Karnali-main are considered. At Q215 (Lalighat), upstream of Karnali-main, observed data for 1995-2004 are available so calibration and validation periods are shorter than for other stations. In Fig. 6a, it is clear that the model is not fully capturing extremes (both high and low flows). The inadequate capturing of low flows holds true for both snowmelt and non-snow melt seasons. Therefore, relatively larger size of the basin (area = 15,200 km$^2$) with only one hydrological station, snowmelt contribution as key source of inflow, but relatively weak snowmelt module of SWAT could be attributed as potential reasons for lower performance on capturing low-flows. Furthermore, the issue is more prominent for the years 1999-2003, whereas low flows is reproduced well for other years as evident from monthly hydrograph. It indicates that data quality can also be a potential reason for overall low performance of the model for the low flows. Similarly, for high flows too, except for few years (e.g., 1997, 1998 2000, and 2004), it is reproduced reasonably. Same reasons for low flows may hold true for low performance in high flows for selected years as well.

There is a wide-range scattering of the observed-simulation dots, indicating relatively weaker performance as well as underestimation of high flows. Nevertheless, average flow conditions are reproduced to a good extent with bias of around 16% (Fig. 6a). The NSE is 0.6 for calibration and more than 0.7 for validation period for daily simulation. The values, at over 0.8, are better for the monthly simulation.

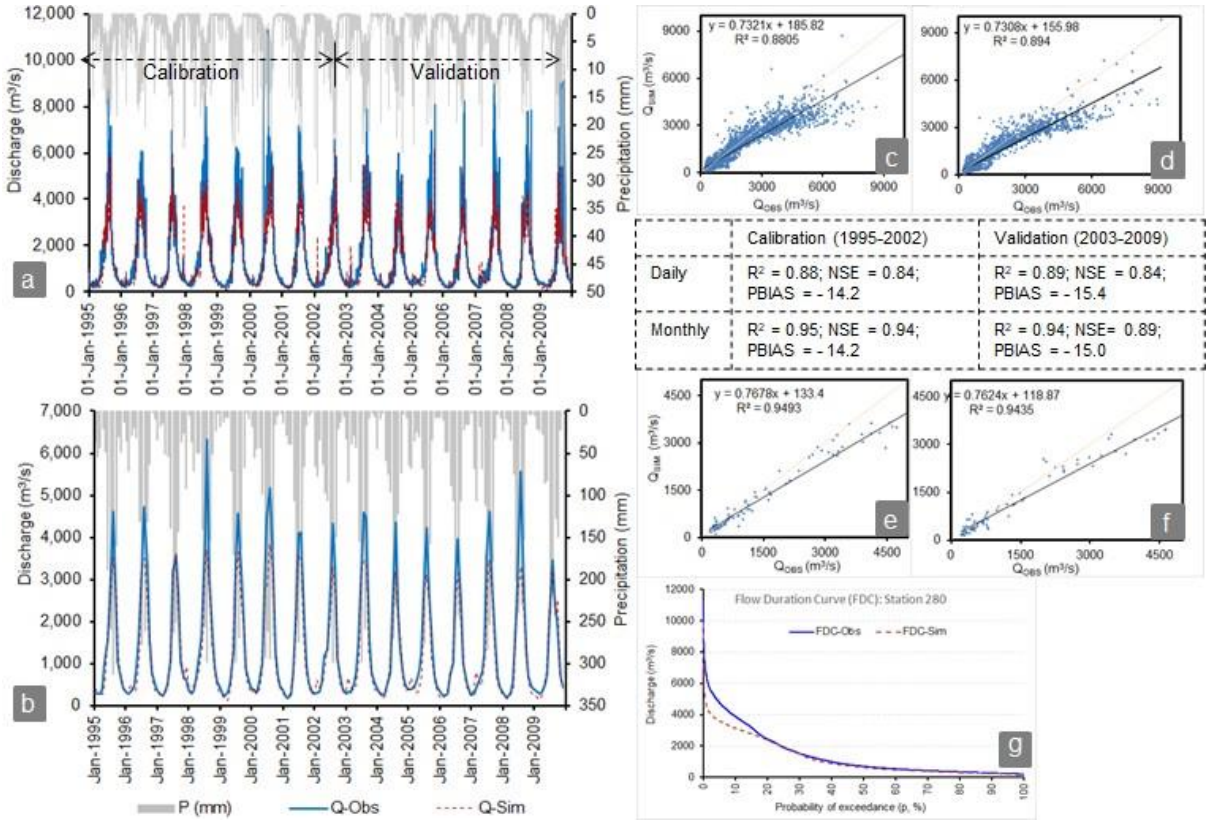


**Figure 5**: Model performance at Q280 (Karnali River) – a) Observed and simulated daily hydrographs; b) Observed and simulated monthly hydrographs; c & d) Scattered plots for daily flow calibration and validation; e & f) Scattered plots for monthly flow calibration and validation; and g) Flow duration curve (FDC, daily).

At the mid-stream of the Karnali-main, i.e., at Q250 (Benighat), daily observed data for the period of 1995-2009 are available. Hydrological patterns for daily and monthly flows are reasonably reproduced. $R^2$ for daily and monthly simulation are 0.83 and 0.91 for calibration and better for validation. NSE values are 0.75 and 0.82 for daily and monthly calibration. Scatter points lie closer to the centerline, but still reflects under-estimation for high flows. As Q250 is at downstream of Q215 in the Karnali-main, the reasons for Q215 holds true for Q250 as well. Therefore, the snowmelt as dominant source of input but relatively weaker snow module in SWAT and data quality could be attributed as potential reasons for note capturing high flows across all the years. The PBIAS for average flow simulation is around -20% for calibration and -24% for validation. Higher bias than upstream station can be expected as errors from upstream sub-basins propagate downstream.

Downstream of the Karnali-main, i.e. at Q280 (Chisapani), daily and monthly flows are simulated for the period of 1995-2009. The simulated hydrographs correspond to the precipitation pattern and reasonably reproduce hydrological regime as well as FDC (Fig. 5). The higher flows are again underestimated, most likely due to cumulative error in the upstream sub-basins. However, average flows are well reproduced with PBIAS of around 15% for both calibration and validation periods. NSE values during calibration are 0.84 for daily and 0.94 for monthly simulation and during validation are over 0.84 for both time scales. Considering all stations along the Karnali-main River, the model is better suited for application based on average flows than for evaluation of extreme events such as high and low flow periods.

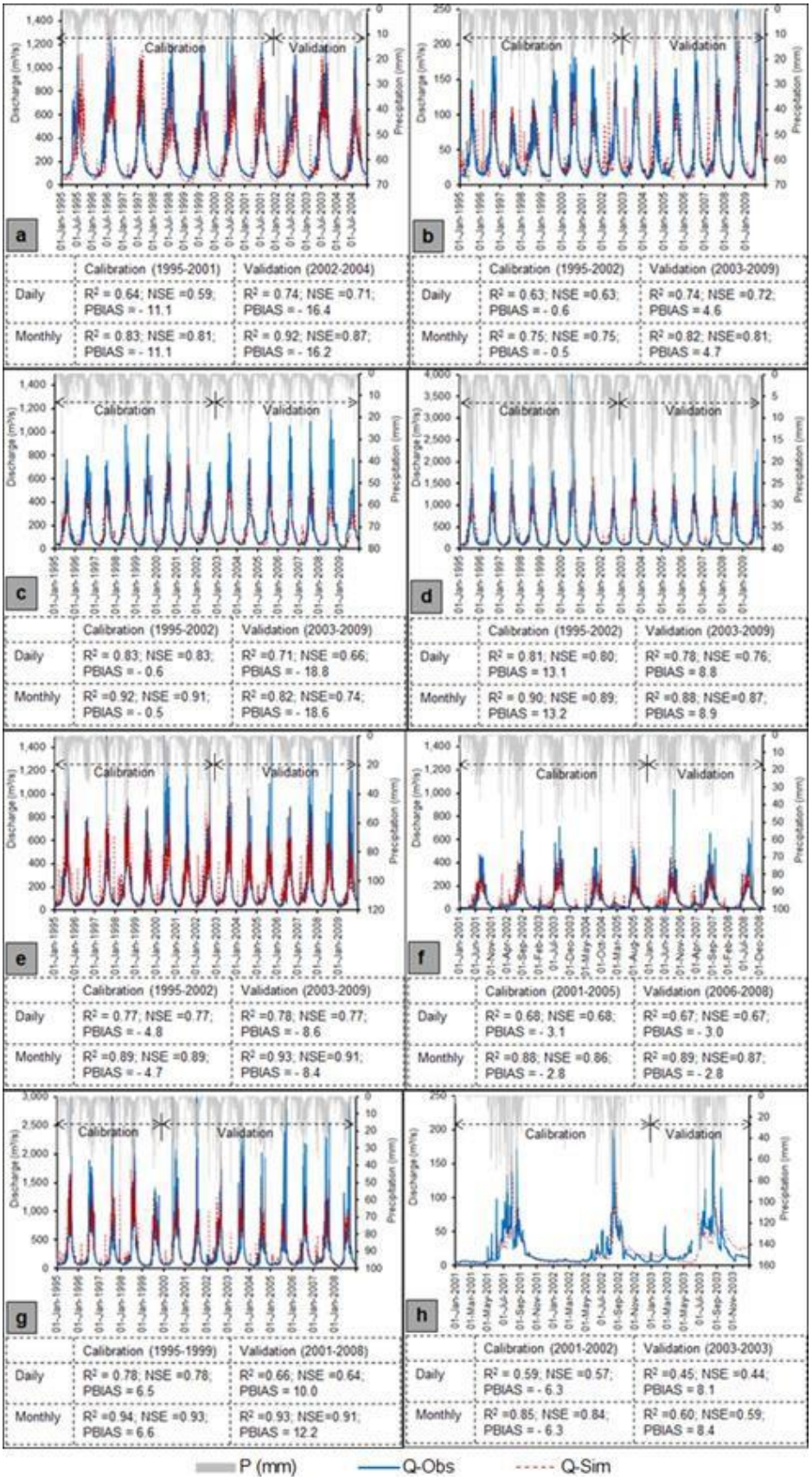


**Figure 6**: Simulated and daily hydrographs and performance indicators at eight hydrological stations in KarMo basin – a) Q215 (Karnali-Main), b) Q220 (Tila), c) Q265 (Thuli Bheri), d) Q270 (Bheri), e) Q259.2 (Seti Upstream), f) Q256.5 (Budhi Ganga), g) Q260 (Seti), and h)

Q283.5 (Pathriya, Mohana)

*4.1.2 Bheri sub-basin*

Simulated hydrographs at the two stations in Bheri sub-basin, upstream at Q265 (Rimna) and downstream at Q270 (Jamu), are comparable with observed, for daily as well as monthly simulations, for the period of 1995-2009. At Q265, as shown in Fig 6c, the long-term average flow is underestimated by less than 1% for calibration and by 18.8% for validation periods. However, mostly high flows are underestimated while low flows are reasonably reproduced. The NSE for calibration and validation of daily flows are 0.83 and 0.66, respectively, with better performance for monthly simulation. The $R^2$ values are also over 0.8 for both calibration and validation. At Q270, as shown in Fig 6d, flow patterns, as indicated by hydrographs and FDC, as well as average flow conditions are well reproduced, with a long-term average bias of only 13% during calibration and 8.8% during validation for the daily flows. The NSE and $R^2$ for all cases are over 0.8 and, except daily validation period; for which, NSE and $R^2$ are 0.76 and 0.78, respectively. As at the stations along the Karnali-main, low and average flow are better simulated than high flows.

*4.1.3 Seti sub-basin*

The SWAT model in the Seti sub-basin is evaluated at three stations located in upstream at Q259.2 (Ghopa Ghat), at Q256.5 (Budhi Ganga), and downstream at Q260 (Bangna) as shown in Fig. 2. At the upstream station Q259.2, simulated hydrographs correspond well to precipitation pattern and reproduce observed daily as well as monthly flows. There is slight underestimation of long-term average flows by less than 5% during calibration and 10% during validation (Fig. 6e). The FDC is well reproduced. The NSE is 0.8 for daily and 0.9 for monthly simulations. The $R^2$ values are also in the same range as NSE. In case of Q256.5 (i.e., in Budhi Ganga), hydrograph patterns as well as FDC are reproduced reasonably with a slight underestimation of long-term average flows by less than 3% for daily as well as monthly simulations (Fig. 6f). The $R^2$ and NSE values are 0.68 for daily simulation and over 0.86 for monthly. However, there is relatively wide scattering of observed-simulated dots, thus reflecting a wider variation in simulated values. At the downstream (Q260), very close to the outlet of Seti, the simulated and observed hydrographs as well as FDCs match closely. Unlike other stations in Karnali and Seti, at Q260 simulations slightly over-estimate long-term average flows by 6.5% during calibration and around 10% during validation (Fig. 6g). The downstream HRUs generate enough runoff to compensate the flow underestimation in upstream, indicating more contribution of the downstream HRUs to the flow at the basin outlet. Land and water management practices in these downstream HRUs, therefore, can have a significant impact on water availability in the sub-basin. The evaluation at three stations suggest that the model is capable of reproducing hydrological regime and average flow conditions in the Seti.

*4.1.4 Mohana sub-basin*

Simulated and observed hydrographs at Q283.5 located in Pathriya, a tributary of Mohana, was made for SWAT performance in Mohana. Very limited reliable data from 2001-2003 is available at this station. Due to the seasonal flash floods in the region, hydrological stations in Mohana have been difficult to maintain and monitor for continuous long-term data as per our personal communication with DHM. As indicated by hydrograph and FDC in Fig. 6h, the flow pattern is reproduced well with long-term average flows underestimated by less than 10% for both daily and monthly simulations The NSE and $R^2$ for calibration are alsoover 0.8 for monthly simulation, even though it drops down to about 0.6 for daily flows. The scattering of simulated-observed dots is very high, which indicates, less reliability in simulated flow pattern across all the seasons even though long-term average is reproduced reasonably. However, considering potential errors in hydrological data collection in the southern rivers like Mohana, the performance can be considered as acceptable.

**Table 3**: Calibrated values of SWAT parameters at 10 stations in five major tributaries in the KarMo basin.

| Parameter | Suggested Range | Bheri | | Seti | | | Karnali-Main | | | Tila | Mohana |
|---|---|---|---|---|---|---|---|---|---|---|---|
| | | Q265 | Q270 | Q259.2 | Q256.5 | Q260 | Q215 | Q250 | Q280 | Q220 | Q283.5 |
| ALPHA_BF | 0 – 1 | 0.60 | 0.66 | 0.80 | 0.50 | 0.50 | 0.10 | 0.90 | 0.90 | 0.40 | 0.95 |
| GW_DELAY | 0 – 500 | 70 | 50 | 15 | 8 | - | 80 | 5 | - | 80 | 200 |
| GW_REVAP | 0.02 – 0.2 | - | - | 0.2 | - | - | - | - | - | - | 0.2 |
| SHALLST | 0 – 50000 | - | - | - | - | - | - | - | - | - | 500 |
| GWQMN | 0 – 5000 | 200 | 200 | 100 | - | - | 500 | 40 | - | - | 5000 |
| RCHRG_DP | 0 – 1 | - | - | - | - | - | - | 0.01 | - | - | 0.1 |
| REVAPMN | 0 – 500 | - | - | 50 | 130 | 261 | - | - | - | - | 100 |
| CANMX | 0 – 100 | 85 | - | 50 | 50 | 63 | 60 | 80 | 70 | 3 | 5 |
| EPCO | 0 – 1 | 0.1 | - | - | - | - | - | - | - | - | 0.1 |
| ESCO | 0 – 1 | 0.98 | 0.20 | - | 0.99 | 0.99 | - | 0.99 | 0.99 | 0.99 | 0.99 |
| LAT_TTIME | 0 – 180 | 80 | 60 | 60 | 35 | 40 | 15 | 100 | - | 70 | 25 |
| SOL_AWC | 0 – 1 | 0.4 | 0.4 | 0.4 | 0.3 | 0.5 | 0.5 | 0.4 | - | 0.3 | - |
| SOL_K | 0 – 2000 | 0.3 | 0.5 | 0.6 | 0.4 | - | 0.6 | 2.0 | - | 0.3 | 2.0 |
| SOL_Z | 0 – 3500 | 0.40 | 0.70 | 2.00 | 0.70 | 0.61 | 0.60 | - | 0.61 | 0.60 | 0.60 |
| CN2 | 35 – 98 | 1.25 | 1.10 | 1.25 | 1.21 | 1.15 | 1.10 | 1.25 | 1.10 | 1.22 | 0.6 |
| CH_K2 | 0 – 500 | 400 | 120 | 104 | 20 | 200 | - | 480 | 104 | 450 | 500 |
| CH_N2 | 0 – 1 | 0.80 | 0.55 | 0.25 | 0.10 | - | 0.50 | 0.56 | - | - | - |
| TLAPS | -10 – 10 | -5.2 | - | -7.1 | -7.5 | -7.1 | -7.1 | 0.0 | - | -2.0 | -9.5 |
| PLAPS | -1000 – 1000 | - | - | 200 | 75 | - | - | 500 | - | - | 50 |
| CH_N1 | 0.01-30 | - | - | - | 10 | - | - | - | - | - | 0.6 |

*Note: Please refer to Table 2 for the definition of parameters. Parameter values not adjusted during calibration are shown as "-". Suggested range is based on SWAT manual*

*4.1.5 Tila sub-basin*

The model performance at Tila is evaluated at Q220 station for the simulation period of 1995-2009. The hydrograph pattern is reproduced satisfactorily with same NSE and $R^2$ values of 0.6 and 0.7 for daily and monthly calibrations, respectively (Fig. 6b). The long-term average flow is slightly underestimated by 0.6% during calibration. The scatter plot indicates good model fit with dots aligned along the central line. The FDC is well reproduced. Compared to other sub-basins, the calibrated SWAT model is capable of reproducing average as well as high flow conditions in the Tila.

**4.2 Spatial distribution of water balance**

Fig. 7 depicts sub-basin wide distribution of major water balance components (average annual P, AET and net water yield) within the KarMo basin as simulated by the model for the hydrological baseline period (1995–2009). The net water yield (NWY) refers to a combination of surface runoff, lateral flow, and groundwater flow, with deduction in transmission losses and pond abstractions (Arnold et al., 1998). The average annual P over the entire basin is 1,375 mm. Net water yield is 927 mm. The average annual AET over the entire basin is 474 mm, which is about 34% of the average annual P. It however, varies across the regions.

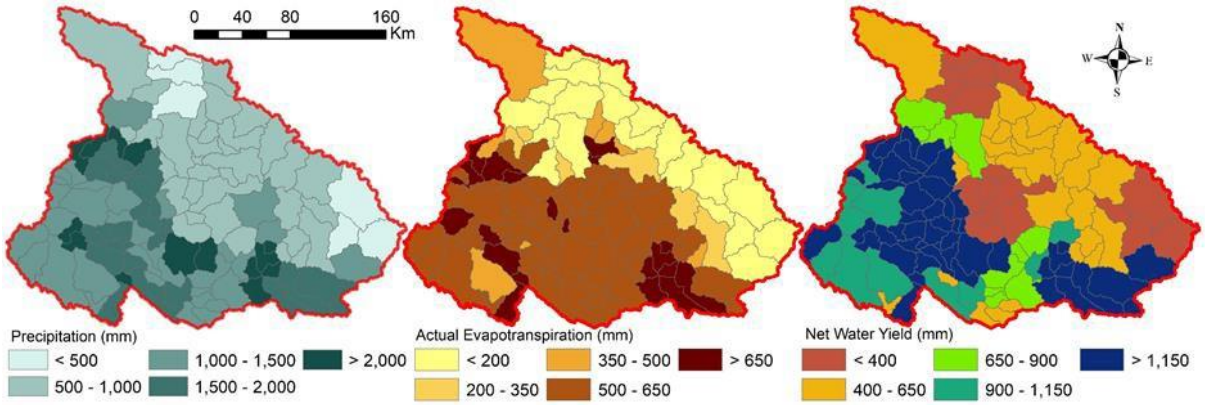


**Figure 7**: Spatial distribution of average annual precipitation (P), actual evapotranspiration (AET) and net water yield (NWY) across sub-basins in Karnali-Mohana basin

The water balance components vary spatially across the sub-basins, with pattern matching the geographical regions of northern Trans-Himalayas (TrH), Mountains (Mnt), Hills (Hil), and southern Tarai flatland, which is a part of Indo-Gangetic Plan (IGP). The precipitation varies from less than 500mm to above 2,000 mm across the 111 sub-basins (Fig. 7a). Fig. 8 depicts variation in the average annual precipitation, AET, and NWY in different geographical regions in the study basin. The error bars indicate the maximum-minimum range for each parameter with the specific region. The Mnt (P = 1,435 mm); Hil (P = 1,625 mm), and IGP (P = 1,566 mm) regions of the basin are relatively wetter compared to the TrH (P = 875 mm) region (Fig. 8). The values of the water balance components across the sub-basins in all the geographical regions vary widely as shown in Fig. 8.

Similarly, the average annual AET across the sub-basins varies from less than 200 mm to over 650 mm (Fig. 7b). The AET value are higher in the Hil (587 mm) and IGP (553 mm) regions, compared to other two regions (Fig. 8), owing to greater area under cultivation and proximity to the oceanfront and equator, especially in case of IGP. Furthermore, due to large forest covers and greenery in the Hil, AET is expected to be higher. The AET decreases as we move to the sub-basins from the southern plains to the northern Trans-Himalayan regions (Fig. 7b) as temperature decreases with altitude. This trend is comparable with the case of Koshi river basin in the eastern Nepal, in which too, AET increases from IGP towards the TrH region (Bharati et al., 2019). The AET in Hil, Mnt, and TrH regions are 587mm, 528 mm, and 227 mm, respectively. The AET as percentage of P in TrH, Mnt, Hil, and IGP regions are 26%, 37%, 36%, and 35%, respectively. The distribution pattern of AET also follows that

of precipitation, which is the major source of moisture in the Western Nepal.

Long-term average NWY in the form of discharge at the sub-basin outlet varies across the sub-basins from 1.1 to 1,357.5 $m^3/s$, where sub-basin areas range from 44 to 3,183 $km^2$. The NWY across the KarMo sub-basins varies from less than 450 mm to above 1,150 mm (Fig. 7c). In terms of geographical regions, the long-term average NWY aggregated over the region decreases as we move upstream from Hil to TrH with values of 1,105 mm in Hil, 961 mm in Mnt, and 587 mm in TrH (Fig. 8).

In fifty (or 45%) sub-basins, NWY are more than 80% of P and in 101 (or 91%) sub-basins the NWY are more than half of P. The surface runoff has the dominant contribution in the net water yield across most of the sub-basins whereas contribution of groundwater and lateral flow varies. Two-third of the sub-basins have more than one-third contribution from surface runoff and rest from other components. In 28% of the sub-basins, contribution of surface runoff is above 50%. The groundwater contribution to the net water yield is less than one-third in 105 (or 94.6%) sub-basins and less than one-quarter in 93 (or 83.8%) sub-basins. It is to be noted that direct comparison in terms of absolute values may not provide critical insights as the sub-basin sizes vary largely from 44 to 3,183 $km^2$.

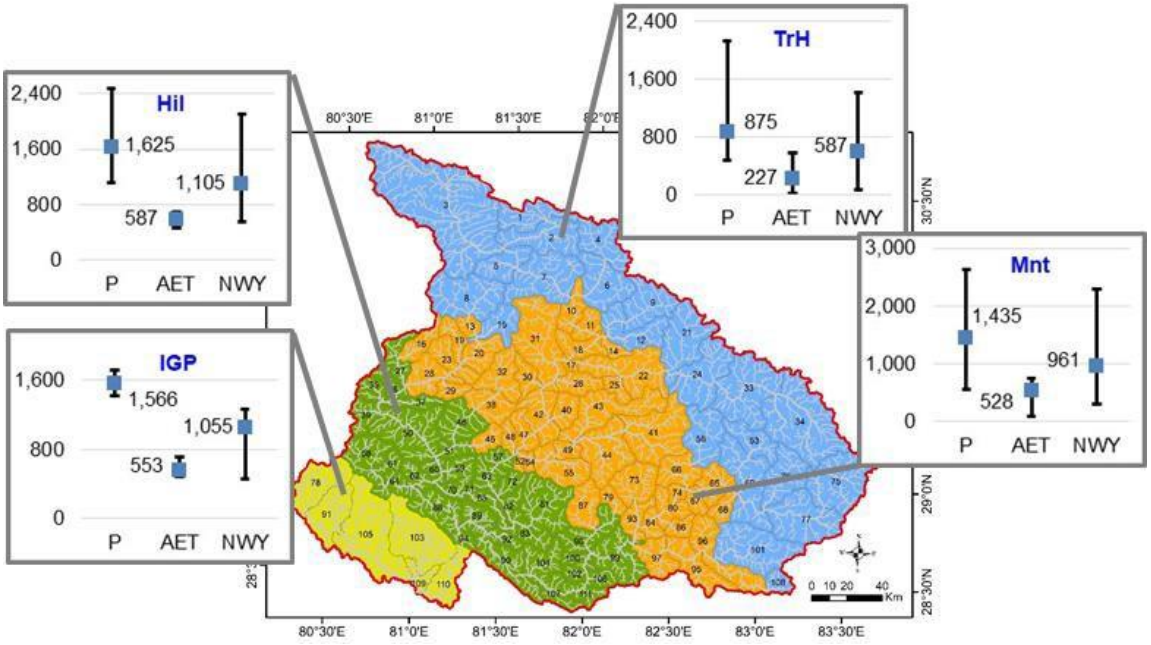


**Figure 8**: Spatial distribution of average annual precipitation (P), actual evapotranspiration (AET) and net water yield (NWY) across geographical regions in Karnali-Mohana basin. TiP is Tibetan Plateau; TrH is Trans-Himalaya; Mnt is Mountain; Hil is Hill; IGP is Indo-Gangetic Plain. The values displayed in the figures are means.

The sum of NWY and AET are different than P in all the regions, primarily because, NWY is not simply the difference between P and AET, but it refers to a combination of surface runoff, lateral flow, and groundwater flow, with deduction in transmission losses and pond abstractions. The net water yield does not always follow the precipitation pattern, but it gets affected by factors such as rainfall intensity, soil properties, and land use/cover characteristics. (Bharati et al., 2019). Therefore, NWY is actually higher than the difference between P and AET in the entire basin as well as some regions (e.g., Mnt, Hil, and IGP) and lower in other region (i.e., TrH), as evident in Fig. 8, due to various reasons. Such issues are evident in other studies as well, such as in the Koshi basin, Eastern Nepal (Bharati et al., 2019). In the TrH region, change in storage – the collective term including groundwater recharge, change in soil moisture storage in the vadose zone and model inaccuracies – is 7% (positive) of the precipitation (rainfall and snowmelt). Ideally, the change in storage in the entire basin as well as regions are supposed to be near to zero, for a long-term average. The positive value of change in storage may reflect that not all the precipitation ina year in the TrH region is

contributing to streamflow; part of that may have been lost in the form of infiltration through steep hills covered with snows, which may re-emerge as lateral flow in the downstream in the basin, and major part of the remaining precipitation could have been stored in the TrH region itself in the form of snow accumulation. Similarly, in Mnt and Hil regions, change in storage are around 4% (negative) of the precipitation, reflecting that NWY is higher than the difference between P and AET. It is likely that the NWY in the Mnt and Hil regions gets contribution from snowmelt and lateral flow emerging from the percolation of precipitation in the TrH region. When moving further downward in the IGP, the southern plain of the basin, the change in storage is still negative but with only 2.7%. In this region, potential contributors to the excess NWY (to P-AET) could be lateral flow as well as fluctuation in groundwater table. As IGP is a part of large groundwater aquifer shared by both India and Nepal, and extends beyond the hydrological boundary, both inflow as well as outflow of groundwater from/to the basin is possible depending upon situation. Finally, average change in storage of the entire basin is 1.9% (negative). The deficit of precipitation in the basin to contribute to NWY might have been compensated from fluctuation in groundwater table, inflow of groundwater from other part of the aquifer extending beyond the KarMo basin boundary, and snowmelt contribution in the upstream of the basin. Though the model results are reasonable at the basin, major sub-basins, as well as a regional scales and useful for planning purpose, model accuracy-related and data-related limitations are certainly embedded in the simulation results. Therefore, results for the small sub-basins located far from the calibration points should be used cautiously because of possible low confidence in results due to calibration and validation of the model at limited number of stations.

### 4.3 Temporal distribution of water balance

The monthly average water balance for the baseline period shows a large temporal variation (Fig. 9). The precipitation (P) is taken as a sum of rainfall and snowmelt. P is taken as observed value while snowmelt, which accounts of 11% of total precipitation, is the model simulated value. Mean seasonal distribution of P in KarMo varies from 68 mm in the post-monsoon (ON) season to 1,098 mm in the monsoon (JJAS). AET is related to P, land use/cover as well as temperature. Mean seasonal distribution of AET in the basin varies from 23 mm in the winter (DJF) season to 290 mm in the monsoon season. And NYW too varies across the season from 72 mm in the winter to 654 mm in the monsoon season. The NWY does not always follow the P patterns because it is also affected by precipitation intensity, soil properties, subsurface storage and land use/cover. For example, rain falling with high intensity on bare and compacted soils will produce higher runoff than longer precipitation events on deep soils and cropped areas (Bharati et al., 2014). The results still show that the monsoon is the main hydrological driver as all the water balance components (i.e. P, AET and NWY) are highest during the monsoon.

The monsoon season (JJAS) contribution is 73%, 61%, and 71% in the average annual P, AET, and NWY, respectively at the KarMo outlet (Fig. 9), which is comparable to values obtained by Bookhagen and Burbanks (2010). As per the results from SWAT simulation, average annual flow volume at the basin outlet under the current climatic scenarios is 46,250 million-cubic-meters (MCM); 71% of which is available during JJAS. The monsoon season contribution varies across the sub-basins, from 63% at the outlet of Q220 to 68% at Q215, 71% at Q270, and 73% at Q260 (please refer Fig. 2 for the locations).

The ‘Δ storage’ is negative in the monsoon (JJAS) season with the absolute value of 17 mm indicating recharge to aquifer (or add to the storage) and positive in the post-monsoon until December, and then becomes negative from January onwards albeit with minimal values. The highest positive value of 91 mm in the post-monsoon (ON) season indicates groundwater contribution to streamflow, which might have appeared as a result of recharge during the monsoon season (JJAS) and discharge of that recharge water in the post-monsoon. Similarly, minimal negative values from January onwards can be explained as the result of winter

precipitation.

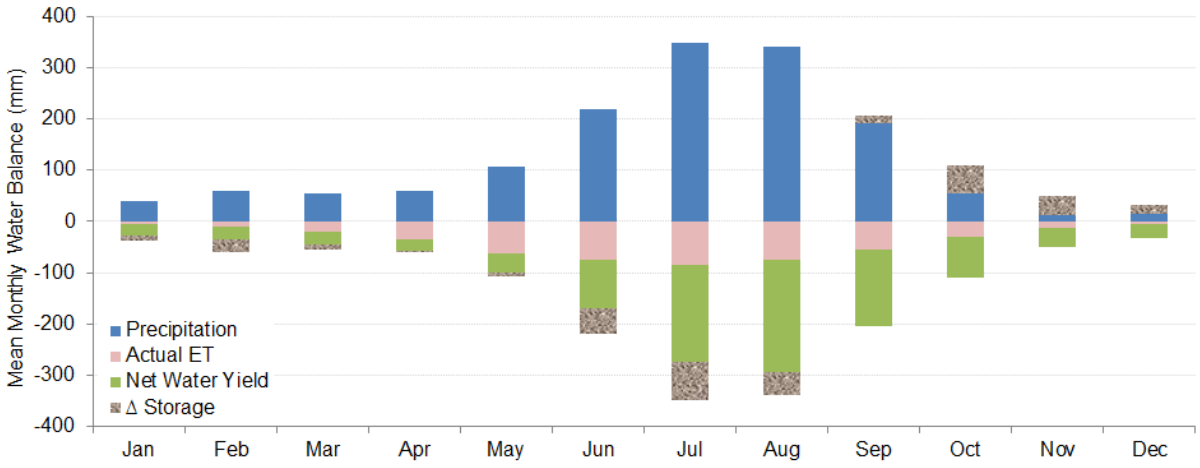


**Figure 9**: Mean monthly simulated (1995-2009) water balance in KarMo basin. The 'Δ storage' is a collective term including groundwater recharge, change in soil moisture storage in the vadose zone and model inaccuracies. Negative (-ve) value of 'Δ storage' indicates recharge to the aquifer and vice-versa.

## 5. CONCLUSIONS

This study discretized the Karnali-Mohana (KarMo) basin in Western Nepal into 111 sub-basins and developed a hydrological model in SWAT using multi-site calibration approach to characterize spatio-temporal distribution in water availability. The model was reasonably calibrated and validated using visual inspection of hydrological pattern as well as statistical indicators for average flows and biases. The annual average precipitation (P) of the KarMo basin is estimated as 1,375 mm and actual evapotranspiration (AET) is 34% (approximately) of the P, but with a large spatio-temporal heterogeneity. The P across the sub-basins vary from less than 500 mm to above 2,000 mm. The Mountain, Hill, and Tarai (a part of Indo-Gangetic Plain) regions are relatively wetter compared to the trans-Himalayan and Tibetan Plateau regions. The AET on the other hand varies from less than 200 mm to over 650 mm, which decreases as we move to the sub-basins from southern plains to the northern Trans-Himalayan regions. And average annual flow volume at the basin outlet under the baseline scenario is 46,250 million-cubic-meters (MCM), and the discharge at the sub-basin outlets vary from 1.1 to 1,357.5 $m^3/s$. Majority of P in most of the sub-basins flow out as river discharge (or net water yield, NWY). The surface runoff has the dominant contribution in NWY across most of the sub-basins whereas contribution of groundwater and later flow varies. In terms of seasons, P varies from 68 mm (post-monsoon) to 1,098 mm (monsoon), AET from 23 mm (winter) to 290 mm (monsoon), and NWY from 72 mm (winter) to 654 mm (monsoon). The monsoon season (JJAS) contribution is 73%, 61%, and 71% in the average annual P, AET, and NWY, respectively at the KarMo outlet.

These model results are adopted for developing national irrigation master plans, estimating environmental flows, and evaluating trade-offs among various future water development pathways. Furthermore, the model is used for climate change impact assessment (Part-B of this paper). The model results are therefore valuable for water resources planners and managers for developing location-specific strategies even within a single basin for sustainable utilization of water resources for the country's prosperity.

**ABBREVIATIONS & ACRONYMS**

AET: Actual Evapotranspiration
BTOPMC: Block-wise use of TOP Model with Muskingum Kung method
CC: Climate change
DEM: Digital Elevation Model
DHM: Department of Hydrology and Meteorology, Government of Nepal
DJB: Digo Jal Bikas
DJF: December-January-February (Winter season)
FDC: Flow Duration Curve
Hil: Hill
HRU: Hydrologic Response Unit
IGP: Indo-Gangetic Plain
IMD: Indian Meteorological Department
JJAS: June-July-August-September (Monsoon season)
KarMo: Karnali-Mohana basin
LH: Latin-Hypercube
LULC: Land use/cover
MAM: March-April-May (Pre-monsoon season)
masl: Meters above the mean sea level
MCM: Million Cubic Meters
mm: Milimeters
Mnt: Mountain
MW: Mega Watts
NASA: National Aeronautics and Space Administration
NSE: Nash-Sutcliffe Efficiency
NWY: Net Water Yield
OAT: One-factor-at-a-time
ON: October-November (Post-monsoon season)
P: Precipitation
PBIAS: Percentage Bias
PET: Potential Evapotranspiration
RH: Relative Humidity
SR: Solar Radiation
SWAT: Soil and Water Assessment Tool
T: Temperature
TiP: Tibetan Plateau
TrH: Trans-Himalayas
TRMM: Tropical Rainfall Measuring Mission
USAID: United States Agency for International Development
WS: Wind Speed

**REFERENCES**

Allen R.G., Pereira L.S., Raes D., Smith M. (1998). Meteorological data – Radiation. In: Crop Evapotranspiration - Guidelines for Computing Crop Water Requirements. FAO Irrigation and Drainage Paper 56, Rome, Italy.

Arnold J.G., Moriasi D.N., Gassman P.W., Abbaspour K.C., White M.J., Srinivasan R., Santhi C., Harmel R.D., Van Griensven A., Van Liew M.W., Kannan N., Jha M.K. (2012). SWAT: model use, calibration, and validation. *Transactions of the American Society of Agricultural and Biological Engineers (ASABE)*, 55(4): 1491-1508.

Arnold J.G., Srinivasan P., Muttiah R.S., Williams J.R. (1998). Large area hydrologic modelling and assessment. Part I. Model development. Journal of American Water Resources Association, 34: 73–89.

Aryal, A., Shrestha, S., & Babel, M. S. (2018). Quantifying uncertainty sources in an ensemble of hydrological climate impact projections. *Theroitical and Applied Climatology*. https://doi.org/doi:10.1029/2011WR011533

Babel, M. S., Bhusal, S. P., Wahid, S. M., & Agarwal, A. (2014). Climate change and water resources in the Bagmati River Basin, Nepal. *Theoretical and Applied Climatology*, *115*(3–4), 639–654.

Bajracharya, A. R., Bajracharya, S. R., Shrestha, A. B., & Maharjan, S. B. (2018). Climate change impact assessment on the hydrological regime of the Kaligandaki Basin, Nepal. *Science of the Total Environment*, *625*, 837–848.

Bharati L., Gurung P., Jayakody P., Smakhtin V., Bhattarai U. (2014). The projected impact of climate change on water availability and development in the Koshi Basin, Nepal. Mountain Research and Development, 34:118–130.

Bharati, L., Gurung, P., Maharjan, L., & Bhattarai, U. (2016). Past and future variability in the hydrological regime of the Koshi Basin, Nepal. *Hydrological Sciences Journal*, *61*(1), 79–93.

Bharati, L.; Bhattarai, U.; Khadka, A.; Gurung, P.; Neumann, L. E.; Penton, D. J.; Dhaubanjar, S.; Nepal, S. 2019. From the mountains to the plains: impact of climate change on water resources in the Koshi River Basin. Colombo, Sri Lanka: International Water Management Institute (IWMI). 49p. (IWMI Working Paper 187). doi: 10.5337/2019.205

Bookhagen B, Burbank DW (2010). Toward a complete Himalayan hydrological budget: Spatiotemporal distribution of snowmelt and rainfall and their impact on river discharge. J Geophys Res 115, F03019. doi: 10.1029/2009JF001426

Devkota, L. P., & Gyawali, D. R. (2015). Impacts of climate change on hydrological regime and water resources management of the Koshi River Basin, Nepal. *Journal of Hydrology: Regional Studies*, *4*, 502–515.

Dhami B., Himanshu S.K., Pandey A., Gautam A.K. (2019). Evaluation of the SWAT model for water balance study of a mountainous snowfed river basin of Nepal. Environmental Earth Sciences, 77: 21.

Dijkshoorn J.A., Huting J.R.M. (2009). Soil and terrain (SOTER) database for Nepal. Report 2009/01, ISRIC – World Soil Information, Wageningen [Online Dataset]. Available at http://www.isric.org/isric/webdocs/docs/ISRIC_Report_2009_01.pdf (Accessed on 15th Dec 2016).

ESA (2015). Climate Change Initiative (CCI) - Land Cover Project: 300 m annual global land cover map from 2015 [Dataset], [online] Available from: http://maps.elie.ucl.ac.be/CCI/viewer/download.php (Accessed 31 August 2016), 2015.

Feldman A.D. (2000). Hydrologic Modeling System HEC-HMS, Technical Reference Manual. U.S. Army Corps of Engineers, Hydrologic Engineering Center, HEC, Davis, CA, USA.

Ghandhari, A., Alavi Moghaddam, S.M.R. (2011). Water balance principles: a review of five watersheds in Iran. J. Environ. Sci. Technol. 4 (5), 465–479.

Gupta H.V., Sorooshian S., Yapo P.O. (1999). Status of automatic calibration for hydrologic models: comparison with multilevel expert calibration. J. Hydrol. Eng., 4 (2): 135–143.

Halwatura D., Najim M.M.M. (2013). Application of the HEC-HMS model for runoff simulation in a tropical catchment. Environmental Modelling & Software, 46: 155-162.

Hasan, M.A., Pradhanang, S.M. (2017). Estimation of flow regime for a spatially varied Himalayan watershed using improved multi-site calibration of the Soil and Water Assessment Tool (SWAT) model. Environ. Earth Sci. 76 (23), 787.

ICIMOD (2010). Land Cover of Nepal 2010 [Dataset]. International Center for Integrated Mountain Development (ICIMOD): Kathmandu, Nepal. Available online at: http://rds.icimod.org/Home/DataDetail?metadataId=9224 [Accessed on 12th January 2017).

IWMI (2018). Annual Report of Digo Jal Bikas (DJB) Project submitted to United States Agency for International Development (USAID). International Water Management Institute (IWMI): Kathmandu, Nepal. April, 2018.

Jeong, J., Kannan, N., Arnold, J., Glick, R., Gosselink, L., & Srinivasan, R. (2010). Development and Integration of Sub-hourly Rainfall-Runoff Modeling Capability Within a Watershed Model. *Water Resources Management*, *24*(15), 4505–4527.

Moriasi D.N., Arnold J.G., van Liew M.W., Bingner R.L., Harmel R.D., Veith T.L. (2007). Model 651 evaluation guidelines for systematic quantification of accuracy in watershed simulations.

Transactions of the ASABE, 50 (3): 885–900.

NASA JPL (2009). Advanced Spaceborne Thermal Emission and Reflection Radiometer (ASTER) Global Digital Elevation Model Version 2 (GDEM V2) [Dataset]. United States National Aeronautics and Space Administration – Jet Propulsion Laboratory (NASA JPL). doi:10.5067/ASTER/ASTGTM.002. (accessed on March 27, 2013)

Nash J.E., Sutcliffe J.V. (1970). River flow forecasting through conceptual models part I – a discussion of principles. J. Hydrol. 10 (3), 282–290.

Nkiaka E., Nawaz N.R., Lovett J.C. (2018). Effect of single and multi-site calibration 660techniques on hydrological l model performance, parameter estimation and predictive uncertainty: a case study in the Logone catchment, Lake Chad basin. Stoch. Environ. Res. Risk Assess., 32: 1665-1682.

Pakhtigian E.L., Jeuland M., Dhaubnjar S., Pandey V.P. (2019). Balancing intersectoral demand in basin-scale planning: The case of Nepal's western river basins. Water Resources Economics. In Press. https://doi.org/10.1016/j.wre.2019.100152

Pandey V.P., Babel M.S., Shrestha S., Kazama F. (2010). Vulnerability of freshwater resources in large and medium Nepalese river basins to environmental change. Water 668 Science and Technology, 61(6): 1525-1534.

Pandey V.P., Dhaubanjar S., Bharati L., Thapa B.R. (2018) Climate Change and Water Availability in Western Nepal. In: Proceedings of National Seminar on Nature for Water. Mar 2018. Nepal Academy of Science and Technology (NAST), Mahendranagar, Nepal. 672 pp 8-19.

Pandey V.P., Dhaubanjar S., Bharati L., Thapa B.R. (2019). Hydrological response of Chamelia watershed in Mahakali Basin to climate change. Science of The Total Environment, 650 (Part 1): 365-383.

Shrestha S., Shrestha M., Babel M.S. (2016). Modeling the potential impacts of climate change on hydrology and water resources in the Indrawati River Basin, Nepal. Environmental Earth Sciences, 75 (4): 1-13

Srinivasan R., Ramanarayanan T.S., Arnold J.G., Bednarz S.T. (1998). Large area hydrological modeling and assessment. Part II: Model application Journal of American Water Resources Association, 34(1): 91-101

Sugawara M. (1979). Automatic calibration of the tank model. Hydrological Sciences Journal, 24 (3): 375-388.

Sunsnik J. (2010). Literature Review and comparative analysis of existing methodologies for water balance, European Commission Seventh Framework (EUFP7) Project.

Takeuchi K, Ao T Q, Ishidaira H (1999). For hydroenvironmental simulation of a large ungauged basin: introduction of block-wise use of TOPMODEL and Muskingum-Cunge method. Hydrological Science Journal, 44(4): 633–646.

Thapa B.R., Ishidaira H., Pandey V.P., Shakya N.M. (2017). A multi-model approach for analysing water balance dynamics in Kathmandu Valley, Nepal. Journal of Hydrology: 691 Regional Studies, 9: 149: 162.

Van Griensven A. (2005). Sensitivity, auto-calibration, uncertainty and model evaluation in SWAT 2005. Unpublished report, 25

**Annex 1**: Description of hydrological stations used in this study

| Index | Lat. (N) | Lon. E) | Elevation (masl) | S. Name | River | Drainage ($km^2$) | Calibration Period | Validation Period |
|---|---|---|---|---|---|---|---|---|
| 215 | 29.159 | 81.591 | 590 | Lalighat | Humla Karnali | 15,200 | 1995 – 2001 | 2002 - 2004 |
| 220 | 29.107 | 81.680 | 1,935 | Nagma | Tila | 1,870 | 1995 – 2002 | 2003 - 2009 |
| 250 | 28.961 | 81.119 | 320 | Benighat | Karnali | 21,240 | 1995 – 2002 | 2003 - 2009 |
| 256.5 | 29.163 | 81.216 | 506 | Chitra | Budhi Ganga | 1,576 | 2001 – 2005 | 2006 – 2008 |
| 259.2 | 29.300 | 80.775 | 750 | Ghopa Ghat | West Seti | 4,420 | 1995 – 2002 | 2003 - 2009 |
| 260 | 28.978 | 81.144 | 328 | Bangna | Seti | 7,460 | 1995 – 1999 | 2001 - 2008 |
| 265 | 28.713 | 82.283 | 550 | Rimna | Thulo Bheri | 6,720 | 1995 – 2002 | 2003 - 2009 |
| 270 | 28.756 | 81.350 | 246 | Jamu | Bheri | 12,290 | 1995 – 2002 | 2003 - 2009 |
| 280 | 28.644 | 81.292 | 191 | Chisapani | Karnali | 42,890 | 1995 – 2002 | 2003 - 2009 |
| 283.5 | 28.504 | 81.054 | 284 | Chhachharawa | Pathariya | 983 | 2001 – 2002 | 2003 - 2003 |

**Annex 2**: Description of meteorological stations used in this study

| Index | S. Name | Lat. (N) | Lon. (E) | Elevation (masl) | Variables | Data Availability (From - To) | | | | |
|---|---|---|---|---|---|---|---|---|---|---|
| | | | | | | P | T (Max, Min) | RH | WS | SH |
| 103 | Patan (West) | 29.467 | 80.533 | 1,266 | P, T, RH | 1956-2015 | 1981-2015 | 1981-2015 | | |
| 104 | Dadeldhura | 29.300 | 80.583 | 1,848 | P, T, RH, WS, SH | 1956-2015 | 1978-2015 | 1978-2015 | 2000-2009 | 1991-2009 |
| 106 | Belapur Shantipur | 28.683 | 80.350 | 159 | P | 1971-2014 | | | | |
| 201 | Pipalkot | 29.617 | 80.867 | 1,456 | P | 1956-2015 | | | | |
| 202 | Chainpur (West) | 29.550 | 81.217 | 1,304 | P, T, RH | 1956-2013 | 1980-2013 | 1980-2013 | | |
| 203 | Silagadhi, Doti | 29.267 | 80.983 | 1,360 | P, T, RH | 1956-2015 | 1987-2015 | 1987-2015 | | |
| 206 | Asara Ghat | 28.950 | 81.450 | 650 | P | 1963-2014 | | | | |
| 207 | Tikapur | 28.533 | 81.117 | 140 | P, T, RH | 1976-2014 | 1976-2014 | 1976-2014 | | |

| | | | | | | | | | | |
|---|---|---|---|---|---|---|---|---|---|---|
| 208 | Sandepani | 28.750 | 80.917 | 195 | P | 1962-2009 | | | | |

| | | | | | | | | | | |
|---|---|---|---|---|---|---|---|---|---|---|
| 209 | Dhangadhi Airport | 28.800 | 80.550 | 187 | P, T, RH, WS, SH | 1956-2015 | 1975-2015 | 1976-2015 | 2000-2015 | 1993-2012 |
| 215 | Godavari (West) | 28.867 | 80.633 | 288 | P, T, RH | 1975-2014 | 1975-2014 | 1976-2014 | | |
| 218 | Dipayal, Doti | 29.252 | 80.946 | 617 | P, T, RH, WS, SH | 1982-2015 | 1982-2015 | 1982-2015 | 2000-2015 | 1999-2012 |
| 302 | Thirpu | 29.317 | 81.767 | 1,006 | P | 1957-2015 | | | | |
| 303 | Jumla | 29.283 | 82.167 | 2,300 | P, T, RH, WS, SH | 1957-2015 | 1970-2015 | 1977-2015 | 2000-2014 | 1991-2014 |
| 304 | Guthi Chaur | 29.283 | 82.317 | 3,080 | P | 1976-2015 | | | | |
| 305 | Sheri Ghat | 29.133 | 81.600 | 1,210 | P | 1966-2015 | | | | |
| 308 | Nagma | 29.200 | 81.900 | 1,905 | P | 1971-2015 | | | | |
| 310 | Dipal Gaon | 29.267 | 82.217 | 2,310 | P, T, RH | 1974-2015 | 1985-2014 | 1987-2014 | | |
| 401 | Pusma Camp | 28.883 | 81.250 | 950 | P, T, RH, WS | 1963-2015 | 1965-2015 | 1976-2015 | 2000-2008 | |
| 402 | Dailekh | 28.850 | 81.717 | 1,402 | P, T, RH | 1957-2015 | 1957-2015 | 1976-2015 | | |
| 405 | Chisapani | 28.650 | 81.267 | 225 | P, T, RH, WS | 1963-2014 | 1965-2013 | 1976-2013 | 2000-2007 | |
| 406 | Surkhet | 28.600 | 81.617 | 720 | P, T, RH, WS, SH | 1957-2015 | 1973-2015 | 1976-2015 | 2000-2014 | 1991-2013 |
| 410 | Balebudha | 28.783 | 81.583 | 610 | P | 1965-2015 | | | | |
| 411 | Rajapur | 28.433 | 81.100 | 129 | P | 1977-2015 | | | | |
| 415 | Bargadaha | 28.433 | 81.350 | 200 | P | 1967-2015 | | | | |
| 417 | Rani Jaruwa Nursery | 28.383 | 81.350 | 200 | P, T, RH | 1976-2015 | 1976-2015 | 1976-2015 | | |
| 501 | Rukumkot | 28.600 | 82.633 | 1,560 | P | 1957-2015 | | | | |
| 511 | Salyan Bazar | 28.383 | 82.167 | 1,457 | P, T, RH | 1960-2015 | 1957-2015 | 1976-2015 | | |
| 513 | Chaur Jhari Tar | 28.633 | 82.200 | 910 | P, T, RH | 1975-2015 | 1979-2015 | 1987-2015 | | |
| 514 | Musikot, Rukumkot | 28.633 | 82.483 | 2,100 | P, T, RH | 1973-2015 | 1981-2015 | 1981-2015 | | |
| 601 | Jomson | 28.783 | 83.717 | 2,744 | P, T, RH | 1957-2015 | 1957-2015 | 1981-2015 | | |
| 604 | Thakmarpha | 28.750 | 83.700 | 2,566 | P, T, RH | 1967-2015 | 1969-2014 | 1976-2014 | | |

| | | | | | | | | | | |
|---|---|---|---|---|---|---|---|---|---|---|
| 607 | Lele | 28.633 | 83.600 | 2,384 | P, T, RH | 1969-2015 | 1998-2015 | 1998-2015 | | |
| 610 | Ghami | 29.050 | 83.883 | 3,465 | P | 1973-2013 | | | | |

| | | | | | | | | |
|---|---|---|---|---|---|---|---|---|
| 615 | Bobang | 28.400 | 83.100 | 2,273 | P | 1978-2015 | | |
| 616 | Gujra Khani | 28.600 | 83.217 | 2,530 | P, T, RH | 1979-2015 | 1999-2014 | 19 |

***Notes**: masl is "meters above mean sea level"; Index is "Station Identification Number of Department of Hydrology and Meteorology, Nepal"; Lat. Is "Latitude"; Lon. Is "Longitude"; S. is "Station"; Q is "River Discharge"; P is "Precipitation"; T is "Temperature"; RH is "Relative Humidity"; All mean five variables (i.e., P, T, RH, sunshine hours, and wind speed).*

**ACKNOWLEDGEMENTS**: This study is made possible by the generous support of the American people through the United States Agency for International Development (USAID) under Digo Jal Bikas (DJB) project. The contents are the responsibility of the authors and do not necessarily reflect the views of USAID or the United States Government.